AGU PUBLICATIONS

Geophysical Research Letters

RESEARCH LETTER
10.1002/2015GL065693

Key Points:
- First direct measurements of hygroscopic properties of dust in the Caribbean
- Dust remained chemically unprocessed and nonhygroscopic despite their long-range transport
- Direct radiative effect of dust was largely independent of RH

Supporting Information:
- Supporting Information S1

Correspondence to:
C. Denjean,
denjean@tropos.de

Citation:
Denjean, C., S. Caquineau, K. Desboeufs, B. Laurent, M. Maille, M. Quiñones Rosado, P. Vallejo, O. L. Mayol-Bracero, and P. Formenti (2015), Long-range transport across the Atlantic in summertime does not enhance the hygroscopicity of African mineral dust, *Geophys. Res. Lett.*, *42*, doi:10.1002/2015GL065693.

Received 6 AUG 2015
Accepted 19 AUG 2015
Accepted article online 21 AUG 2015

Long-range transport across the Atlantic in summertime does not enhance the hygroscopicity of African mineral dust

C. Denjean[1,2], S. Caquineau[3], K. Desboeufs[1], B. Laurent[1], M. Maille[1], M. Quiñones Rosado[4], P. Vallejo[4], O. L. Mayol-Bracero[4], and P. Formenti[1]

[1]Laboratoire Interuniversitaire des Systèmes Atmosphériques, UMR-CNRS 7583, Université Paris-Est-Créteil et Université Paris Diderot, Institut Pierre-Simon Laplace, Créteil, France, [2]Leibniz Institute for Tropospheric Research (TROPOS), Leipzig, Germany, [3]IRD-Sorbonne Universités (UPMC, University of Paris 06)-CNRS-MNHN, LOCEAN Laboratory, IRD France-Nord, Bondy, France, [4]Department of Environmental Science, University of Puerto Rico, San Juan, Puerto Rico

Abstract We present the first direct evidence that the hygroscopic properties of super micron (>1 μm) African dust particles did not change despite undergoing long-range transport across the Atlantic toward the Caribbean. Concurrent measurements of chemical composition show that most of mineral dust was chemically unprocessed and externally mixed. A minor portion of mineral dust was internally mixed with sulfate and chloride (~13–24% by number) or aggregated with sea-salt particles (~3–6%). Only dust particles aggregated with sea salt showed significant hygroscopic growth above 75% relative humidity (RH), resulting in a decrease in extinction mass efficiency by up to a factor 2.2. All other dust particles did not take up significant amounts of water when exposed to up to 94% RH. These results demonstrate that the direct radiative effect of African dust in this region remained independent of RH and an external mixing state could be considered for evaluating the climate effects of dust.

1. Introduction

Mineral dust is an extremely important atmospheric constituent because of its remarkable global influence on climate [*Huneeus et al*., 2011]. Dust particles affect the Earth's radiative budget directly via the scattering and absorption of solar and terrestrial radiation [*di Sarra et al*., 2011]. Mineral dust can also have an indirect effect on cloud radiative properties by acting as cloud condensation nuclei (CCN) and ice nuclei (IN) [*Choobari et al*., 2014]. Since the interaction of particles with water changes their size, composition, and shape, and henceforth their optical properties, these radiative effects are strongly sensitive to the hygroscopicity of particles.

While fresh mineral dust is highly nonhygroscopic, a number of laboratory studies have indicated that the uptake of hydrophilic species, such as sulfuric acid, nitric acid, or oxidized organic species, by the dust surface can enhance its hygroscopicity [*Hatch et al*., 2008; *Sullivan et al*., 2009]. Soluble coatings on dust have been observed in the atmosphere during field measurements [*Matsuki et al*., 2010; *Li and Shao*, 2009; *Falkovich et al*., 2004]. Coagulation of dust with hygroscopic particles such as ammonium sulfate or sodium chloride has also been documented in the past [*Sullivan et al*., 2007; *Trochkine et al*., 2003]. Therefore, dust hygroscopic properties may change as the dust undergoes atmospheric processing during long-range transport. An accurate description of the temporal evolution of dust hygroscopic properties is crucial to quantify dust impact on the climate system that is a challenge for models [*Smoydzin et al*., 2012].

Findings in the literature about dust hygroscopic properties show different results and are partly contradictory. Several studies have reported coating-induced enhancements in the hygroscopic properties of Saharan and Asian dust transported over a long range [*Bègue et al*., 2014; *Twohy et al*., 2009; *Perry et al*., 2004; *Matsuki et al*., 2010]. By contrast, *Pósfai et al*. [2013] provided evidence that although Saharan dust particles were transported over long distances (more than 3 days), their chemical composition can remain unaltered after transport, with no observed internal mixing or coating. Nonhygroscopic Asian dust particles were also observed in Chinese outflow [*Massling et al*., 2007]. Hence, the extent to which mineral dust particles react and become hydrophilic is dictated by their origin and transport pathway and may differ from one area to another depending on meteorological conditions and air masses encountered. Further studies that analyze

dust hygroscopic properties after long-range transport in various regions are needed to accurately model the impact of dust on climate.

Large quantities of mineral dust are transported westward from North African desert source regions toward the Caribbean and the eastern coasts of North and South America [*Prospero and Mayol-Bracero*, 2013]. Most previous studies in this region have focused on the analysis of dust microphysical, chemical, and optical properties under ambient conditions [*Maring et al*., 2003; *Reid et al*., 2003; *Trapp et al*., 2010]. To date, only one publication has addressed the influence of relative humidity on the scattering properties of transported dust and found that only minor amounts of hygroscopic materials were associated with dust [*Li-Jones et al*., 1998].

Here we present direct measurements of the hygroscopic properties of Saharan mineral dust collected in Puerto Rico after its long-range transport across the Atlantic Ocean. We show that long-range transport did not result in changes in dust hygroscopicity and discuss the implications of these results for dust radiative effects.

2. Methods

2.1. Samples

Aerosol samples were collected during the Dust Aging and Transport from Africa to the Caribbean (Dust-ATTACk) campaign, which was conducted in summer 2012 at the atmospheric observatory of Cabezas de San Juan (CPR, 18°23′N, 65°37′W) in Fajardo, Puerto Rico. Puerto Rico is a Caribbean island dominated by northeasterly winds, which carry high concentrations of dust from Africa to this region [*Gioda et al*., 2011], particularly during the boreal summer. Previous studies have also reported the presence of significant anthropogenic organic and sulfate fractions in this region, which are indicators of local and transported pollution from Europe [*Allan et al*., 2008; *Li-Jones and Prospero*, 1998].

For the purposes of this study, a four-stage cascade impactor (Dekati®, four-size range including >10, 2.5 to 10, 1 to 2.5, <1 μm) was used to collect particles for microscopy study. Particles were collected on scanning electron microscopy (SEM) Cu grids mounted on nonhygroscopic polytetrafluoroethylene filters. The samples presented here were collected under two contrasting sets of conditions: (1) dusty conditions during an intense dust event, on 2 July 2012, and (2) regional background conditions during a transition period between two dust events, on 29 June 2012. Dust source regions were identified from the aerosol indexes derived from the Ozone Monitoring Instrument aboard the EOS-Aura platform and from numerical simulations of dust emissions using the dust production model developed by *Marticorena and Bergametti* [1995]. During the dust event, mineral dust was emitted from Mauritania, Western Sahara and Central Algeria in 24–25 June and reached Puerto Rico after 6–8 days of transport, as shown in Figure S1 in the supporting information.

2.2. ESEM Analysis

Environmental scanning electron microscopy (ESEM) was used to analyze the size, shape, chemical composition, and hygroscopic properties of individual particles having diameters larger than 1 μm. High-resolution images of the particles were obtained using a ZEISS Evo® LS15 scanning electron microscope. An acceleration voltage of 15 kV and a beam current between 300 and 400 pA were used for the analysis. The particles were identified on the basis of their elemental spectrum, which was obtained with an energy dispersive X-ray microprobe (EDX, Oxford Instruments, INCA Energy 350) at a relative humidity (RH) below 5%. Lighter elements (C, N, and O) and Cu from the SEM grids were excluded for the classification of the particles. A total of 450 particles were analyzed. Particles selected for analysis were separated by more than 1 μm such that when deliquescing, they would not come into physical contact.

Particle hygroscopic properties were determined using a differentially pumped environmental chamber by examining the particle growth and phase transitions as a function of RH. The deliquescence point corresponds to the RH at which particles take up water to form a solution droplet. Samples were initially dried and then hydrated in a stepwise fashion. The RH in the chamber was incrementally increased by introducing a controlled amount of water vapor and by progressively increasing the pressure in the chamber. At each RH step, high-resolution images of each selected particle were taken. In order to ensure that equilibrium was reached, sample images were taken 5 min after stabilization of each RH level, and we checked that no change in particle size and shape occurred during this time.

Table 1. Contribution of Mineral Dust to the Number of Coarse-Mode Particles and Contribution of Sulfate-, Chloride-, and NaCl-Containing Dust Particles to the Number of Mineral Dust Particles

Samples Information				Externally Mixed Particles (%)			Mixing of Mineral Dust (%)		
Conditions	Sampling Date	Sampling Time	No. of Particles	Dust	NaCl	Metallic	S Bearing	Cl Bearing	NaCl Aggregate
Dust event	2/7/2012	10:36–13:57	280	84	11	5	9	4	6
Regional background	29/6/2012	16:10–18:50	170	69	5	26	21	3	3

Samples were kept at a constant temperature using a Peltier stage as a control element and a diode to measure the sample temperature. ESEM analysis was performed at 4 ± 1°C, which allowed for a maximum RH of 94 ± 5%. At RH values above 94%, water condensed on the filters, making pressure and temperature in the sample chamber difficult to control. Therefore, no water uptake analyses above 94% RH are presented here. Prior to the analysis of ambient particles, RH in the sample chamber was controlled by measuring the hygroscopic growth and deliquescence point of laboratory-generated ammonium sulfate particles.

2.3. Optical Models

Aerosol optical properties relevant to radiative transfer (mass extinction efficiency, k_{ext}; single-scattering albedo, ω_0; and asymmetry factor, g) were calculated as a function of RH using a discrete dipole approximation (DDA) model, DDSCAT version 7.3 [*Draine and Flatau*, 2008]. For the calculation, 3-D shapes of particles were discretized into an array of dipoles with individual polarizabilities, as shown in Figure S2 in the supporting information. Particle size and growth at different RH were determined from their ESEM images assuming the cross-sectional diameter equal to the volume equivalent diameter. Using these parameters, 3-D particles having compact aggregated spheres with distinct refractive indexes were simulated. All DDA computations were performed using more than 100,000 dipoles for a particle.

Mie calculations of individual particles were also performed to determine k_{ext}, ω_0, and g using homogeneous mixing and core-shell models [*Bohren and Huffman*, 1983] and assuming spherical single particles having the same volume as used in DDA calculations. Refractive indexes of mixed components were determined from their volume-weighted refractive indexes, based on the particle growth and phase transitions observed during ESEM measurements, as further detailed in the supporting information. DDA and Mie calculations were both performed at 550 nm wavelength.

3. Results

3.1. Mixing State of Mineral Dust Particles

During the Dust-ATTACk campaign, aerosol volume size distributions were dominated by a well-defined coarse mode (Figure S3 in the supporting information), which contributed between 65% (regional background conditions) and 80% (dust event) of the total particle volume concentration. Particles with diameters smaller than 1 μm were not observed on the ESEM images under dry conditions because of the instrument detection limit. However, the accumulation mode particles were centered between 600 and 800 nm, and hydrophilic dust particles in this size range should have been detected after taking up water. Above 75% RH, occurrence of accumulation mode particles was observed on the ESEM images, but all these particles exhibited the same deliquescence point and hygroscopic behavior as NaCl particles. No significant hygroscopic growth arising from dust particles in the accumulation mode was observed in this study.

Based on the EDX-ESEM analysis, coarse-mode (diameter > 1 μm) particles in Puerto Rico samples consisted of mineral dust, sea-salt, and metallic particles. Dust particles were defined as those containing at least one of Si, Al, Ca, or Fe. Sea-salt particles were recognized by their cubic/rectangular prism shape and the detection of both Na and Cl. Metallic particles were rich in Zn, Pb, or Cr, indicating a probable anthropogenic origin. Particles identified as mineral dust were divided into three subgroups, depending on the relative contribution of the characteristic elements: aluminosilicates for particles characterized by the dominance of Al and Si, quartz (SiO_2) for those having only Si as major element, and calcite ($CaCO_3$) for those enriched in Ca. The contribution of each particle type is listed in Table 1. Dust particles contributed ~84% of the coarse-mode particle number concentration during the dust event and ~69% under regional background conditions.

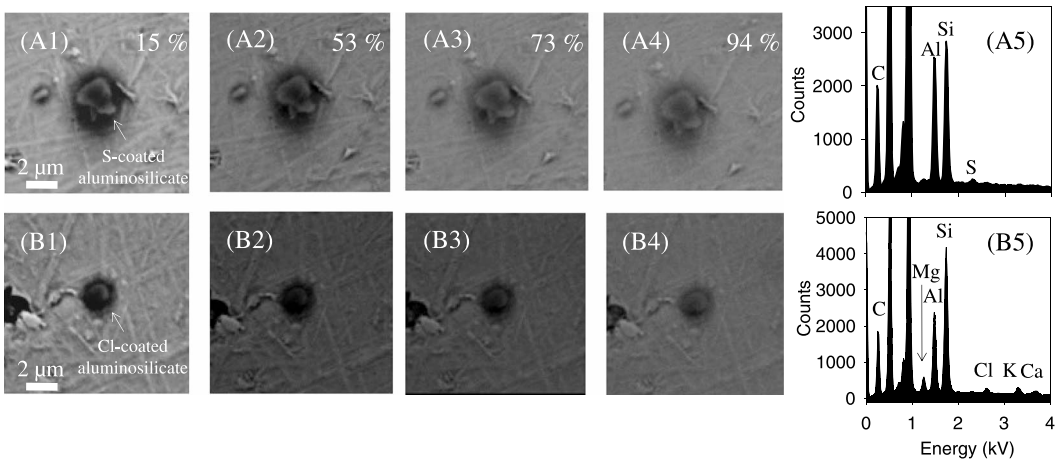

Figure 1. ESEM images of (a) sulfate-coated dust particles and (b) chloride-coated dust particles exposed to increasing relative humidity (1–4) at $T = 5$°C. EDS spectra of these particles are shown in Figures 1a5 and 1b5.

These results suggest that the local atmosphere was loaded under both conditions with large dust particles, which were mixed during their transport with particles of marine and urban/industrial origins.

Aluminosilicate particles represented the majority (88%) of the 450 dust particles analyzed. Quartz and calcite accounted for 7% and 5% of the dust particles analyzed, respectively. Only 19–27% (by number) of the dust particles studied with the ESEM were internally mixed, all of which were aluminosilicates. Based on their EDX spectrum, these particles were divided into three categories: S bearing, Cl bearing, and NaCl aggregated. Most of the mixing detected on aluminosilicate particles were associated with S, which is consistent with laboratory studies suggesting that sulfate coatings are favored on aluminosilicates rather than on calcium carbonates [*Shi et al*., 2008]. Our observations of Cl-bearing aluminosilicate particles are somewhat surprising, since calcium-rich particles have previously been considered to be the most reactive with HCl [*Tobo et al*., 2010]. The uptake of chloride to form chloride coating could be the result of heterogeneous chemistry with chloride precursor gases liberated from sea-salt particles [*Sullivan et al*., 2007]. Only a small fraction of mineral dust was found to be mixed with sea-salt particles, which confirms previous observations showing that dust–seasalt aggregation occurs only to a minor degree in the African plume outflow during its transport over Atlantic Ocean [*Reid et al*., 2003]. The EDX-ESEM analysis did not reveal the presence of N-bearing dust particles in our samples, which indicates that mineral dust contained no or low amount of nitrate. Previous laboratory and field studies have shown that nitrate coatings are favored on calcite particles [*Shi et al*., 2008; *Sullivan et al*., 2007]. Since calcite represented only a minor portion of the dust particles analyzed, most of mineral dust transported in the Caribbean was not expected to react readily with nitric acid. In addition, the altitude of transport of mineral dust from the Saharan desert to marine environment in the Caribbean could also explain this observed trend in dust mixing state.

The altitude of dust transport was estimated using 5 day back trajectory calculations performed with the HYSPLIT (Hybrid Single-Particle Lagrangian Integrated Trajectory) model and the Global Data Assimilation System [*Draxler and Rolph*, 2015] and observations from the Cloud-Aerosol Lidar with Orthogonal Polarization (CALIOP) carried on the CALIPSO satellite [*Winker et al*., 2009]. As shown in Figure S4 in the supporting information, these estimates indicate that the dust transport within the marine boundary layer (MBL) was limited to 1 day before reaching the CPR station; previously, dust transport occurred mostly in high-altitude layers above 1.5 km. The low mixing of dust with sea-salt particles was likely due to the dust transport at high altitudes during summertime [*Peyridieu et al*., 2013]. Moreover, the data showed that no potentially polluted European air masses reached Puerto Rico during the sampling period, which suggests that the mixing of dust with acidic gases is also limited during its transport as polluted air masses are not involved.

3.2. Water Uptake of S- and Cl-Bearing Mineral Dust Particles

Figure 1 shows ESEM images and EDX spectra of S- and Cl-bearing dust particles. Although the mixings are not physically apparent, they can be identified using the signals of S and Cl detected by the EDX analysis.

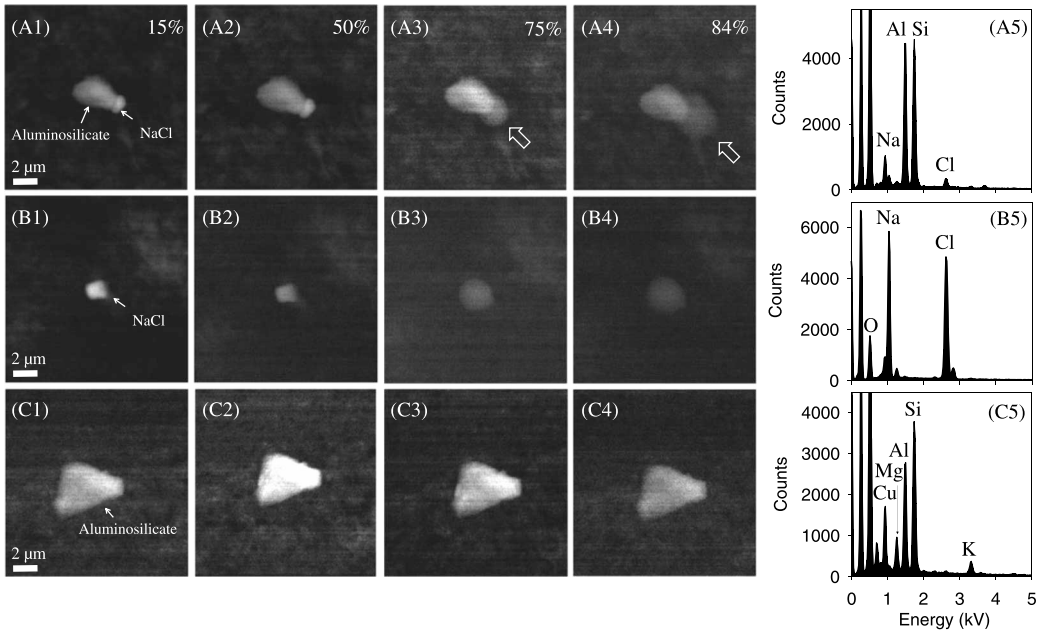

Figure 2. ESEM images of (a) NaCl aggregated to dust particles, (b) relatively pure NaCl, and (c) relatively pure aluminosilicate exposed to increasing relative humidity (1–4) at $T = 5°C$. EDS spectra of these particles are shown in Figures 2a5, 2b5, and 2c5.

As shown in this figure, the morphology of both sulfate- and chloride-containing dust particles did not change appreciably when exposed to RH values of up to 94%. Henceforth, internally mixed mineral dust remained nonhygroscopic; i.e., the S and Cl bearing did not enhance the water uptake capacity of the dust.

There are several potential explanations for this behavior. First, the heterogeneous reaction of sulfate with dust may not lead to an increase of the water uptake under subsaturated conditions: previous studies have shown that mineral dust particles containing sulfate did not experience hygroscopic growth at 90% RH, which might be due to the presence of alkaline elements in these particles [*Shi et al*., 2008; *Ma et al*., 2012]. Second, as shown in Figure 1, the S and Cl mixing were not visible in the ESEM images, and the signals of S and Cl in the EDX spectra were low. This suggests low concentrations of sulfate and chloride on the surface of the dust particles. Finally, these mineral dust particles could also contain other insoluble species not detected by EDX, such as organic compounds. The hygroscopic properties of organic species are not well understood and depend strongly on their chemical nature. If insoluble organic compounds are present as surface films on soluble particles, the particle water uptake could be reduced [*Meyer et al*., 2009]. The presence of dust-associated organic compounds cannot be confirmed from our analysis, however, since organics readily decompose when exposed to an electron beam.

3.3. Water Uptake of Dust Aggregated With NaCl Particles

Figure 2a shows the hygroscopic behavior of an aluminosilicate particle partly attached to a soluble NaCl crystal. Particles were exposed to a RH that was increased from 5 to 94% in the ESEM. No change in morphology occurred as the RH increased from 5 to 75% RH. At 75% RH, however, deliquescence of the NaCl aggregate occurred, according to the same pattern of deliquescence as ambient NaCl (Figure 2b). The droplet formed a large exterior sphere attached to the aluminosilicate particle. As the RH increased to 94% RH, this droplet grew adjacent to the aluminosilicate particle and partially engulfed the dust particle. Except for the slight change in morphology due to this partial covering, the dust aggregate did not show more morphological changes, as was observed for the nonhygroscopic aluminosilicate (Figure 2c). Therefore, our results indicate that the hygroscopic growth of mineral dust in our samples is controlled by the deliquescence of NaCl aggregated to the dust surface and that the resulting deliquesced particles were not spherical, as previously observed by *Wise et al*. [2007], *Semeniuk et al*. [2007], and *Freney et al*. [2010].

4. Atmospheric Implications

The majority of transported dust particles did not show hygroscopic growth up to 94% RH, indicating that most dust particles were chemically unprocessed and externally mixed. The heterogeneous reaction of sulfate and chloride has only a minor effect on the hygroscopic properties of mineral dust. The main hygroscopic growth of mineral dust arose from water uptake by aggregated NaCl particles.

We represent the impact of water uptake on particle size by plotting the hygroscopic growth factor (GF), defined as the ratio of the particle diameter at a given RH to the particle diameter at 5% RH, for each particle type. Particle diameters were determined from the projected 2-D area assumed as the equivalent area of a spherical particle, as further detailed in the supporting information. As shown in Figure 3a, GF was calculated for 29 NaCl particles, 50 S- and Cl-bearing dust particles, and 10 agglomerates of dust and NaCl. The measured GF for NaCl was compared with theoretical calculations based on the Köhler equations. Although deriving hygroscopic growth from 2-D ESEM images may overestimate the calculated GF, values retrieved for ambient NaCl particles were close to the theoretical values. Therefore, we are confident in applying this approach to determine the GF of mineral dust particles. We determined that the aggregation of mineral dust with NaCl particles was associated with an enhancement of the dust hygroscopicity, with a GF of 1.77 at 90% RH.

Figures 3b–3d show k_{ext}, ω_0, and g at a wavelength of 550 nm calculated from the size of individual particles at different RH, the contribution of each particle type and by employing different optical models. As we observed that most of mineral dust survived atmospheric transport intact, we assumed a refractive index and a density for mineral dust of $1.53 - 0.002i$ and $2.6\,g\,cm^{-3}$, respectively, which correspond to averages of the values reported in African source region, as discussed in the supporting information. For NaCl, we used values of $1.54 - 0.000i$ and $2.2\,g\,cm^{-3}$ for the refractive index and the density, respectively [*Tang and Munkelwitz*, 1994; *Hess et al*., 1998].

The k_{ext} of dust aggregated with NaCl decreased from 1.90 to $0.85\,m^2\,g^{-1}$ between 75% and 94% RH using DDA calculation, most likely due to the mutual shadowing among particles. These values were lower by up to 2.2 times than those obtained using volume-mixing and core-shell models. This indicates that the assumption employed in widely used optical models that deliquesced particles have spherical shapes could lead to a significant overestimation of the dust radiative effect. No significant change with RH in ω_0 of dust aggregated with NaCl was observed. NaCl particles are non absorbing (ω_0 equal to unity). Therefore, dust mixed with NaCl particles is expected to have ω_0 equal or higher than those of pure dust particles. Optical parameters of the overall dust aerosol population were calculated using values for single dust particles and the contribution of each particle mixing state. We estimate that k_{ext}, ω_0, and g of the integrated dust aerosol population were $1.90\,m^2\,g^{-1}$, 0.97, and 0.9, respectively, regardless of RH values. Similar results were obtained for dusty and background conditions (not shown). Although dust particles in the accumulation mode were also observed during the Dust-ATTACk campaign (Figure S3 in the supporting information), our measurements were limited to supermicronic ($>1\,\mu m$) particles, which represented the dominant fraction of dust mass. Supermicronic particles being the main contributors to the aerosol light absorption, we may have overestimated k_{ext} and underestimated ω_0 relative to that in the atmosphere. However, our results clearly show that the enhancement of dust hygroscopicity was counterbalanced by the limited fraction of dust aggregated with sea-salt particles. The direct radiative effect of African dust after its long-range transport over the Atlantic Ocean was independent of RH.

5. Conclusions

This work provided the first direct evidence that supermicronic dust particles remained externally mixed and nonhygroscopic despite undergoing long-range transport over the Atlantic Ocean. The heterogeneous reaction of sulfate and chloride had only a minor effect on the hygroscopic properties of mineral dust. The main hygroscopic growth was measured when NaCl particles were aggregated with mineral dust. However, the enhancement of dust hygroscopicity was counterbalanced by the limited fraction of dust aggregated with sea-salt particles.

These findings are crucial for determining the impact of dust on climate. The arid regions of North Africa are the most prolific and persistent sources of mineral dust at the global scale, and the trans-Atlantic dust

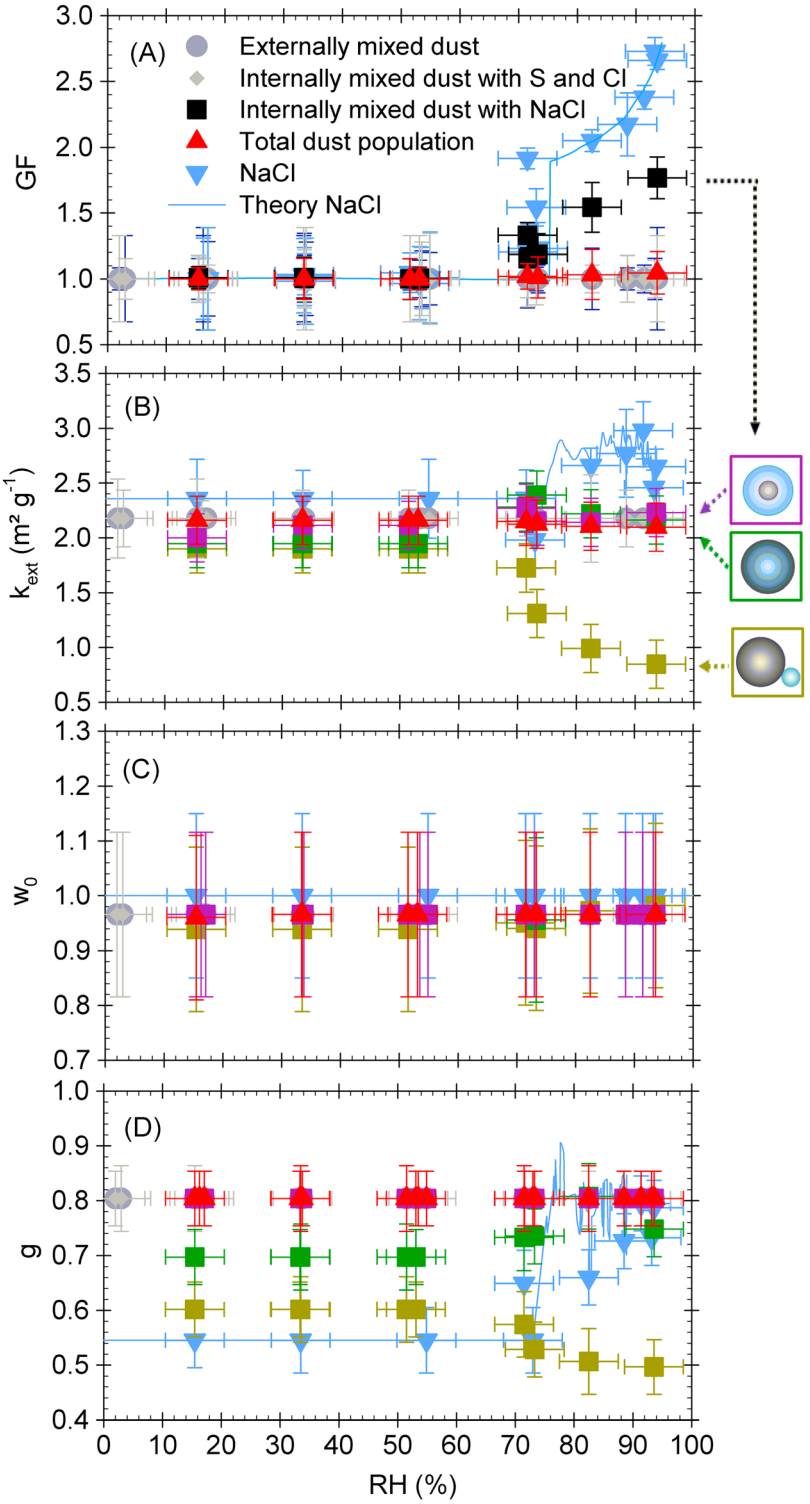

Figure 3. (a) Hygroscopic growth factor (GF), (b) scattering mass efficiency (k_{ext}), (c) single-scattering albedo (ω_0), and (d) asymmetry parameter (g) at $\lambda = 550$ nm as a function of relative humidity for each particles type. Externally mixed dust particles, i.e., S, Cl, and Na, were not detected and are shown in dark grey circles, dust internally mixed with sulfate or chloride in grey diamonds, and relatively pure NaCl particles in blue triangles. Dust aggregated with NaCl particles is shown in black squares in Figure 3a and is separated for the different dust mixing state with NaCl in Figure 3b, with green squares representing the homogeneous mixing, purple squares for the core-shell mixing, and golden squares for the aggregate structure. GF and k_{ext} of the total dust population (red triangles) were calculated using GF and k_{ext} values of single dust particles and the contribution of each particle type.

transport impacts large geographical areas in summertime [*Liu et al*., 2008]. On the basis of our measurements, we demonstrated that the direct radiative effect of African dust in the Caribbean was independent of RH. Nonetheless, despite their nonhygroscopicity under subsaturated conditions, mineral dust can act as efficient CCN and IN due to their relatively large size [*Choobari et al*., 2014] and can have important implications for microphysical properties and precipitation efficiency of clouds. The CCN and IN properties of mineral dust are intimately linked to dust mixing state. In general, it was found that the condensation or coagulation of soluble compounds, such as sulfuric acid, on mineral dust increased CCN activity and reduced deposition IN activation [*Sullivan et al*., 2009; *Augustin-Bauditz et al*., 2014]. As dust particles in our samples remained mostly unaffected by atmospheric processing, our results suggest that an external mixing state should be considered in evaluating the climate effects of dust.

The study presented in this paper focused on a single Saharan dust event sampled along the east coast of Puerto Rico. The conclusions drawn from this investigation are, however, likely to be relevant to dust events in summertime in the Caribbean. From 5 years ground-based measurements, *Prospero and Mayol-Bracero* [2013] reported a remarkable repeatability of the mass concentration of dust from Africa in the Caribbean in summertime, suggesting that the contribution of mineral dust to the air mass is probably quite similar for the different dust events uncounted in the Caribbean. Previous studies showed that the chemical composition of dust is rather uniform at Puerto Rico [*Trapp et al*., 2010; *Reid et al*., 2003] with almost no contribution of anthropogenic aerosols [*Allan et al*., 2008], making this site attractive for studying the properties of aerosol in pristine marine environment. As the Saharan trans-Atlantic transport in summertime occurs mostly in the Saharan Air Layer above the MBL [*Peyridieu et al*., 2013], a low degree of internal mixing of dust with sea-salt particles is expected. Nevertheless, further field investigations for longer-term period and in different locations are required to determine how frequently mineral dust is externally mixed and remains nonhygroscopic after long-range transport across the Atlantic. Long-term sampling projects and systematic ESEM-EDX analysis would go a long way to addressing the dust mixing state and hygroscopicity in order to improve the representation of dust in climate models.

Acknowledgments

We thank the Conservation Trust of Puerto Rico for allowing the use of their facilities at the natural reserve of Cabezas de San Juan. This project was funded by the Partner University Fund, a program of the French Embassy in the United States, and the FACE Foundation. We also acknowledge the support of the National Science Foundation (NSF GEO AGS 0936879 grant), the Institute for Tropical Ecosystem Studies and the Department of Environmental Science at the University of Puerto Rico Rio Piedras Campus, the International Institute of Tropical Forestry USDA Forest Service, and the Luquillo Long-Term Ecological Research Program. ESEM data were obtained at the ALYSES facility (IRD-UPMC), which is supported by grants from Région Ile-de-France. We thank the NOAA Air Resources Laboratory (ARL) for the HYSPLIT transport and dispersion models and the READY website (http://ready.arl.noaa.gov) used in this study. We acknowledge the NASA Langley CALIOP team and the ICARE data center for the CALIOP data. We warmly thank Sarah Styler (Leibniz Institute for Tropospheric Research, Germany) for her helpful revision of the manuscript. We gratefully acknowledge the reviewers whose suggestions helped improve and clarify this manuscript.

The Editor thanks two anonymous reviewers for their assistance in evaluating this paper.

References

Allan, J. D., et al. (2008), Clouds and aerosols in Puerto Rico—A new evaluation, *Atmos. Chem. Phys.*, *8*, 1293–1309, doi:10.5194/acp-8-1293-2008.

Augustin-Bauditz, S., H. Wex, S. Kanter, M. Ebert, D. Niedermeier, F. Stolz, A. Prager, and F. Stratmann (2014), The immersion mode ice nucleation behavior of mineral dusts: A comparison of different pure and surface modified dusts, *Geophys. Res. Lett.*, *41*, 7375–7382, doi:10.1002/2014GL061317.

Bègue, N., P. Tulet, J. Pelon, B. Aouizerats, A. Berger, and A. Schwarzenboeck (2014), Aerosol processing and CCN formation of an intense Saharan dust plume during the EUCAARI 2008 campaign, *Atmos. Chem. Phys. Discuss.*, *14*, 27,039–27,091, doi:10.5194/acpd-14-27039-2014.

Bohren, C. F., and D. R. Huffman (1983), *Absorption and Scattering of Light by Small Particles*, Wiley, New York.

Choobari, O. A., P. Zawar-Reza, and A. Sturman (2014), The global distribution of mineral dust and its impacts on the climate system: A review, *Atmos. Res.*, *138*, 152–165, doi:10.1016/j.atmosres.2013.11.007.

di Sarra, A., C. Di Biagio, D. Meloni, F. Monteleone, G. Pace, S. Pugnaghi, and D. Sferlazzo (2011), Shortwave and longwave radiative effects of the intense Saharan dust event of 25–26 March 2010 at Lampedusa (Mediterranean Sea), *J. Geophys. Res.*, *116*, D23209, doi:10.1029/2011JD016238.

Draine, B. T., and P. J. Flatau (2008), Discrete-dipole approximation for periodic targets: Theory and tests, *J. Opt. Soc. Am. A*, *25*, 2693–2703, doi:10.1364/JOSAA.25.002693.

Draxler, R. R., and G. D. Rolph (2015), HYSPLIT (HYbrid Single-Particle Lagrangian Integrated Trajectory) model, NOAA Air Resources Lab., Silver Spring, Md. [Available at http://ready.arl.noaa.gov/HYSPLIT.php.]

Falkovich, A. H., G. Schkolnik, E. Ganor, and Y. Rudich (2004), Adsorption of organic compounds pertinent to urban environments onto mineral dust particles, *J. Geophys. Res.*, *109*, D02208, doi:10.1029/2003JD003919.

Freney, E. J., K. Adachi, and P. R. Buseck (2010), Internally mixed atmospheric aerosol particles: Hygroscopic growth and light scattering, *J. Geophys. Res.*, *115*, D19210, doi:10.1029/2009JD013558.

Gioda, A., G. J. Reyes-Rodríguez, G. Santos-Figueroa, J. L. Collett, S. Decesari, M. C. K. V. Ramos, H. J. C. Bezerra Netto, F. R. de Aquino Neto, and O. L. Mayol-Bracero (2011), Speciation of water-soluble inorganic, organic, and total nitrogen in a background marine environment: Cloud water, rainwater, and aerosol particles, *J. Geophys. Res.*, *116*, D05203, doi:10.1029/2010JD015010.

Hatch, C. D., K. M. Gierlus, J. D. Schuttlefield, and V. H. Grassian (2008), Water adsorption and cloud condensation nuclei activity of calcite and calcite coated with model humic and fulvic acids, *Atmos. Environ.*, *42*, 5672–5684, doi:10.1016/j.atmosenv.2008.03.005.

Hess, M., P. Koepke, and I. Schult (1998), Optical properties of aerosols and clouds: The software 8 package OPAC, *Bull. Am. Meteorol. Soc.*, *79*, 831–844, doi:10.1175/1520-0477(1998)079<0831:OPOAAC>2.0.CO;2.

Huneeus, N., et al. (2011), Global dust model intercomparison in AeroCom phase I, *Atmos. Chem. Phys.*, *11*, 7781–7816, doi:10.5194/acp-11-7781-2011.

Li, W. J., and L. Y. Shao (2009), Observation of nitrate coatings on atmospheric mineral dust particles, *Atmos. Chem. Phys.*, *9*, 1863–1871, doi:10.5194/acp-9-1863-2009.

Li-Jones, X., and J. M. Prospero (1998), Variations in the size distribution of non-sea-salt sulfate aerosol in the marine boundary layer at Barbados: Impact of African dust, *J. Geophys. Res.*, *103*(D13), 16,073–16,084, doi:10.1029/98JD00883.

Li-Jones, X., H. B. Maring, and J. M. Prospero (1998), Effect of relative humidity on light scattering by mineral dust aerosol as measured in the marine boundary layer over the tropical Atlantic Ocean, *J. Geophys. Res.*, *103*, 31,113–31,121, doi:10.1029/98JD01800.

Liu, D., Z. Wang, Z. Liu, D. Winker, and C. Trepte (2008), A height resolved global view of dust aerosols from the first year CALIPSO lidar measurements, *J. Geophys. Res.*, *113*, D16214, doi:10.1029/2007JD009776.

Ma, Q. X., Y. C. Liu, C. Liu, and H. He (2012), Heterogeneous reaction of acetic acid on MgO, alpha-Al_2O_3, and $CaCO_3$ and the effect on the hygroscopic behaviour of these particles, *Phys. Chem. Chem. Phys.*, *14*, 8403–8409, doi:10.1039/c2cp40510e.

Maring, H., D. L. Savoie, M. A. Izaguirre, L. Custals, and J. S. Reid (2003), Mineral dust aerosol size distribution change during atmospheric transport, *J. Geophys. Res.*, *108*(D19), 8592, doi:10.1029/2002JD002536.

Marticorena, B., and G. Bergametti (1995), Modelling the atmospheric dust cycle: 1. Design of a soil derived dust production scheme, *J. Geophys. Res.*, *100*, 16,415–16,430, doi:10.1029/95JD00690.

Massling, A., S. Leinert, A. Wiedensohler, and D. Covert (2007), Hygroscopic growth of sub-micrometer and one-micrometer aerosol particles measured during ACE-Asia, *Atmos. Chem. Phys.*, *7*, 3249–3259, doi:10.5194/acp-7-3249-2007.

Matsuki, A., A. Schwarzenboeck, H. Venzac, P. Laj, S. Crumeyrolle, and L. Gomes (2010), Cloud processing of mineral dust: Direct comparison of cloud residual and clear sky particles during AMMA aircraft campaign in summer 2006, *Atmos. Chem. Phys.*, *10*, 1057–1069, doi:10.5194/acp-10-1057-2010.

Meyer, N. K., et al. (2009), Analysis of the hygroscopic and volatile properties of ammonium sulphate seeded and unseeded SOA particles, *Atmos. Chem. Phys.*, *9*, 721–732.

Perry, K. D., S. S. Cliff, and M. P. Jimenez-Cruz (2004), Evidence for hygroscopic mineral dust particles from the Intercontinental Transport and Chemical Transformation Experiment, *J. Geophys. Res.*, *109*, D23S28, doi:10.1029/2004JD004979.

Peyridieu, S., et al. (2013), Characterisation of dust aerosols in the infrared from IASI and comparison with PARASOL, MODIS, MISR, CALIOP, and AERONET observations, *Atmos. Chem. Phys.*, *13*, 6065–6082, doi:10.5194/acp-13-6065-2013.

Pósfai, M., D. Axisa, É. Tompa, E. Freney, R. Bruintjes, and P. R. Buseck (2013), Interactions of mineral dust with pollution and clouds: An individual-particle TEM study of atmospheric aerosol from Saudi Arabia, *Atmos. Res.*, *122*, 347–361, doi:10.1016/j.atmosres.2012.12.001.

Prospero, J. M., and O. L. Mayol-Bracero (2013), Understanding the transport and impact of African dust on the Caribbean Basin, *Bull. Am. Meteorol. Soc.*, *94*, 1329–1337, doi:10.1175/BAMS-D-12-00142.1.

Reid, E. A., J. S. Reid, M. M. Meier, M. R. Dunlap, S. S. Cliff, A. Broumas, K. Perry, and H. Maring (2003), Characterization of African dust transported to Puerto Rico by individual particle and size segregated bulk analysis, *J. Geophys. Res.*, *108*(D19), 8591, doi:10.1029/2002JD002935.

Semeniuk, T., M. Wise, S. Martin, L. Russell, and P. Buseck (2007), Hygroscopic behavior of aerosol particles from biomass fires using environmental transmission electron microscopy, *J. Atmos. Chem.*, *56*, 259–273, doi:10.1007/s10874-006-9055-5.

Shi, Z., D. Zhang, M. Hayashi, H. Ogata, H. Ji, and W. Fujiie (2008), Influences of sulfate and nitrate on the hygroscopic behaviour of coarse dust particles, *Atmos. Environ.*, *42*, 822–827, doi:10.1016/j.atmosenv.2007.10.037.

Smoydzin, L., A. Teller, H. Tost, M. Fnais, and J. Lelieveld (2012), Impact of mineral dust on cloud formation in a Saharan outflow region, *Atmos. Chem. Phys.*, *12*, 11,383–11,393, doi:10.5194/acp-12-11383-2012.

Sullivan, R. C., S. A. Guazzotti, D. A. Sodeman, and K. A. Prather (2007), Direct observations of the atmospheric processing of Asian mineral dust, *Atmos. Chem. Phys.*, *7*, 1213–1236, doi:10.5194/acp-7-1213-2007.

Sullivan, R. C., M. J. K. Moore, M. D. Petters, S. M. Kreidenweis, G. C. Roberts, and K. A. Prather (2009), Effect of chemical mixing state on the hygroscopicity and cloud nucleation properties of calcium mineral dust particles, *Atmos. Chem. Phys.*, *9*, 3303–3316.

Tang, I. N., and H. R. Munkelwitz (1994), Water activities, densities, and refractive indexes of 33 aqueous sulfates and sodium-nitrate droplets of atmospheric importance, *J. Geophys. Res.*, *99*, 18,801–18,808, doi:10.1029/94JD01345.

Tobo, Y., D. Zhang, A. Matsuki, and Y. Iwasaka (2010), Asian dust particles converted into aqueous droplets under remote marine atmospheric conditions, *Proc. Natl. Acad. Sci. U.S.A.*, *107*, 17,905–17,910, doi:10.1073/pnas.1008235107.

Trapp, J. M., F. J. Millero, and J. M. Prospero (2010), Temporal variability of the elemental composition of African dust measured in trade wind aerosols at Barbados and Miami, *Mar. Chem.*, *120*, 71–82, doi:10.1016/j.marchem.2008.10.004.

Trochkine, D., Y. Iwasaka, A. Matsuki, M. Yamada, Y. S. Kim, T. Nagatani, D. Zhang, G. Y. Shi, and Z. Shen (2003), Mineral aerosol particles collected in Dunhuang, China, and their comparison with chemically modified particles collected over Japan, *J. Geophys. Res.*, *108*(D23), 8642, doi:10.1029/2002JD003268.

Twohy, C. H., et al. (2009), Saharan dust particles nucleate droplets in eastern Atlantic clouds, *Geophys. Res. Lett.*, *36*, L01807, doi:10.1029/2008GL035846.

Winker, D. M., M. A. Vaughan, A. Omar, Y. X. Hu, K. A. Powell, Z. Y. Liu, W. H. Hunt, and S. A. Young (2009), Overview of the CALIPSO mission and CALIOP data processing algorithms, *J. Atmos. Oceanic Technol.*, *26*, 2310–2323, doi:10.1175/2009jtecha1281.1.

Wise, M. E., T. A. Semeniuk, R. Bruintjes, S. T. Martin, L. M. Russell, and P. R. Buseck (2007), Hygroscopic behavior of NaCl-bearing natural aerosol particles using environmental transmission electron microscopy, *J. Geophys. Res.*, *112*, D10224, doi:10.1029/2006JD007678.